

SPECTROSCOPIC CONFIRMATION OF A MASSIVE RED-SEQUENCE-SELECTED GALAXY CLUSTER AT $z = 1.34$ IN THE SpARCS-SOUTH CLUSTER SURVEY

GILLIAN WILSON¹, ADAM MUZZIN², H. K. C. YEE³, MARK LACY⁴, JASON SURACE⁴, DAVID GILBANK⁵, KRIS BLINDERT⁶, HENK HOEKSTRA^{7,8,14}, SUBHABRATA MAJUMDAR⁹, RICARDO DEMARCO¹, JONATHAN P. GARDNER¹⁰, MICHAEL D. GLADDERS¹¹, AND CAROL LONSDALE^{12,13}

¹ Department of Physics and Astronomy, University of California, Riverside, CA 92521, USA; gillianw@ucr.edu

² Department of Astronomy, Yale University, New Haven, CT 06520-8101, USA

³ Department of Astronomy and Astrophysics, University of Toronto, 50 St. George Street, Toronto, ON M5S 3H4, Canada

⁴ Spitzer Science Center, California Institute of Technology, 220-6, Pasadena, CA 91125, USA

⁵ Astrophysics and Gravitation Group, Department of Physics and Astronomy, University Of Waterloo, Waterloo, ON N2L 3G1, Canada

⁶ Max Planck Institute for Astronomy Koenigstuhl 17, 69117 Heidelberg, Germany

⁷ Department of Physics and Astronomy, University of Victoria, Victoria, BC V8P 5C2, Canada

⁸ Leiden Observatory, Leiden University, P.O. Box 9513, 2300RA Leiden, The Netherlands

⁹ Department of Astronomy and Astrophysics, Tata Institute of Fundamental Research (TIFR), Homi Bhabha Road, Mumbai, India

¹⁰ Goddard Space Flight Center, Code 665, Laboratory for Observational Cosmology, Greenbelt, MD 20771, USA

¹¹ Department of Astronomy and Astrophysics, University of Chicago, 5640 South Ellis Avenue, Chicago, IL 60637, USA

¹² Infrared Processing and Analysis Center, California Institute of Technology, 220-6, Pasadena, CA 91125, USA

¹³ North American ALMA Science Center, NRAO Headquarters, 520 Edgemont Road, Charlottesville, VA 22903, USA

Received 2008 September 30; accepted 2009 April 13; published 2009 June 5

ABSTRACT

The *Spitzer* Adaptation of the Red-sequence Cluster Survey (SpARCS) is a z' -passband imaging survey, consisting of deep ($z' \simeq 24$ AB) observations made from both hemispheres using the CFHT 3.6 m and CTIO 4 m telescopes. The survey was designed with the primary aim of detecting galaxy clusters at $z > 1$. In tandem with pre-existing 3.6 μm observations from the *Spitzer Space Telescope* SWIRE Legacy Survey, SpARCS detects clusters using an infrared adaptation of the two-filter red-sequence cluster technique. The total effective area of the SpARCS cluster survey is 41.9 deg². In this paper, we provide an overview of the 13.6 deg² Southern CTIO/MOSAIC II observations. The 28.3 deg² Northern CFHT/MegaCam observations are summarized in a companion paper by Muzzin et al. In this paper, we also report spectroscopic confirmation of SpARCS J003550–431224, a very rich galaxy cluster at $z = 1.335$, discovered in the ELAIS-S1 field. To date, this is the highest spectroscopically confirmed redshift for a galaxy cluster discovered using the red-sequence technique. Based on nine confirmed members, SpARCS J003550–431224 has a preliminary velocity dispersion of 1050 ± 230 km s⁻¹. With its proven capability for efficient cluster detection, SpARCS is a demonstration that we have entered an era of large, homogeneously selected $z > 1$ cluster surveys.

Key words: cosmology: observations – galaxies: clusters: general – galaxies: high-redshift – infrared: galaxies – surveys

Online-only material: color figures

1. INTRODUCTION

Dating back to the pioneering photographic work of the mid-twentieth century (Abell 1958; Zwicky et al. 1968), galaxy cluster surveys have held a special place in the history of astronomy. Due to the limitations of photographic plates, however, early optical surveys struggled to discover clusters at redshifts higher than $z \simeq 0.2$.

Galaxy cluster surveys were revolutionized by the launch of a series of powerful X-ray observatories in the 1980's and 1990's. Firstly *Einstein*, then *ROSAT*, and later the *XMM-Newton* and *Chandra* telescopes proved their capability to detect clusters out to $z = 1$. For example, the wide but relatively shallow 734 deg² *Einstein* Extended Medium-Sensitivity Survey (EMSS; Gioia et al. 1990) both provided the base catalog for the Canadian Network for Observation Cosmology (CNOC1) survey of clusters at $z \sim 0.4$ (Yee et al. 1996), and discovered MS 1054-03 at $z = 0.83$ (Gioia & Luppino 1994), a massive cluster which provided the first evidence that Ω_m was significantly < 1 (Donahue et al. 1998). The deeper but smaller 48 deg² *ROSAT* Deep Cluster Survey (RDCS; Rosati et al. 1998) detected RX J0848.9+4452

at $z = 1.26$, which was, at the time, one of the most distant clusters to be discovered (Rosati et al. 1999).

The advent of large-format charge-coupled devices (CCDs) brought renewed interest in carrying out optical cluster surveys e.g., the 6 deg² Palomar Distant Cluster Survey (PDCS; Postman et al. 1996), the 16 deg² KPNO survey of Postman et al. (1998), and the 135 deg² Las Campanas Distant Cluster Survey (LCDCS; Gonzalez et al. 2001) from which the ESO Distant Cluster Survey (EDisCS; White et al. 2005) was selected. All three of these surveys used variants of the matched-filter method to detect clusters.

In an effort to combat “false positive” detections caused by line-of-sight projections of unrelated systems in single-passband optical cluster searches, Gladders & Yee (2000) proposed a two-filter technique. Their Cluster Red-Sequence (CRS) technique was motivated by the observational fact that galaxy clusters contain a population of early-type galaxies which follow a tight color–magnitude relation. This relation has been shown to have an extremely small scatter (e.g., Bower et al. 1992), even to redshifts as high as $z \sim 1.4$ (Blakeslee et al. 2003; Holden et al. 2004; Lidman et al. 2008; Mei et al. 2009). If two filters which bracket the 4000 Å break are used to construct color–magnitude diagrams, early types are always the brightest,

¹⁴ Alfred P. Sloan Fellow

reddest galaxies at any redshift, and provide significant contrast from the field. The CRS method has been used for the ~ 100 deg² Red-sequence Cluster Survey (RCS-1; Gladders & Yee 2005) and is also being used for the next generation ~ 1000 deg² RCS-2 survey (Yee et al. 2007). Both of these surveys use an $R - z'$ filter combination. A variant of the red sequence method (the BCGmax algorithm) has also been used to detect clusters in the Sloan Digital Sky Survey (Koester et al. 2007a, 2007b). In addition to detecting clusters with a very low false-positive rate, a second important advantage of the CRS technique is that it also provides a good photometric estimate of the cluster redshift, accurate to $\Delta z \sim 0.05$ at $z < 1$ (Gilbank et al. 2007).

Applying the CRS technique to searching for clusters at higher redshift was an obvious next step which was not feasible until very recently, because of technical limitations. At $z \sim 1.2$, the z' filter is no longer redward of the rest-frame 4000 Å break, requiring the use of large-format near-infrared cameras which have only recently begun to appear on 4 m telescopes (Dalton et al. 2006; Warren et al. 2007). Another issue is that the sky itself is bright in the infrared, requiring longer integration times than for optical imaging.

The first real opportunity to systematically detect galaxy clusters at $z > 1$ in large numbers was presented in 2003 with the launch of the Infrared Array Camera (IRAC; Fazio et al. 2004) onboard the *Spitzer Space Telescope* (Werner et al. 2004). Both our own pilot study carried out using the 3.8 deg² 60 s depth First Look Survey (FLS; Lacy et al. 2005; Wilson et al. 2006; Muzzin et al. 2008), and that carried out using the 8.5 deg² 90 s depth IRAC Shallow Survey (Eisenhardt et al. 2004, 2008; Stanford et al. 2005; Brodwin et al. 2006), quickly demonstrated the power of IRAC for $z > 1$ cluster detection.

Clusters of galaxies are extremely rare and one requires a widefield survey to find the most massive examples. The largest area *Spitzer* Survey is the 50 deg² 120 s depth SWIRE Legacy Survey (Lonsdale et al. 2003). In Section 2, we provide an overview of SpARCS,¹⁵ our z' -imaging survey of the six SWIRE fields. We also summarize the southern observations. In Section 3, we briefly review our red-sequence detection algorithm and introduce a rich cluster candidate, SpARCS J003550–431224, selected in the CTIO ELAIS-S1 field. We present Gemini/GMOS-S spectroscopic follow-up of SpARCS J003550–431224 in Section 4, confirming it to be, at $z = 1.34$, the highest redshift cluster yet discovered using the red-sequence technique. We discuss our main results in Section 5 and conclude in Section 6. We assume an $\Omega_m = 0.3$, $\Omega_\Lambda = 0.7$ cosmology with $H_0 = 70$ km s⁻¹ Mpc⁻¹ throughout.

2. SPARCS SURVEY IMAGING

2.1. Choice of Passbands

The *Spitzer* SWIRE Legacy Survey is a seven passband imaging survey consisting of IRAC 3.6, 4.5, 5.8, 8.0 μ m and Multiband Imaging Photometer for *Spitzer* (MIPS; Rieke et al. 2004) 24, 70, 160 μ m observations. Full details of the survey design, data processing, ancillary data sets, and source catalogs may be found in Surace et al. (2005). For cluster detection SpARCS utilizes 3.6 μ m, the most sensitive *Spitzer* channel, as its “red” filter.

SpARCS utilizes z' as its “blue” filter. Simulations (e.g., see Wilson et al. 2008) showed a limiting magnitude of $z \sim 24$

Table 1
SpARCS Fields

Field	R.A. J2000	Decl. J2000	SWIRE 3.6 μ m Area (deg ²)	SpARCS z' Area (deg ²)	Usable Area (deg ²)
ELAIS-S1 ^a	00:38:30	−44:00:00	7.1	8.3	6.5
XMM-LSS	02:21:20	−04:30:00	9.4	11.7	7.3
Chandra-S ^a	03:32:00	−28:16:00	8.1	7.9	7.1
Lockman	10:45:00	+58:00:00	11.6	12.9	9.7
ELAIS-N1	16:11:00	+55:00:00	9.8	10.3	7.9
ELAIS-N2	16:36:48	+41:01:45	4.4	4.3	3.4
Total			50.4	55.4	41.9

Note.

^a CTIO field.

AB was required to match the 3.6 μ m depth. It was necessary to obtain our own widefield z' -imaging for only five of the six SWIRE fields (Table 1), because observations of the XMM-LSS field were available from the CFHT Legacy Survey.¹⁶ Those observations were made either using the MOSAIC II instrument on the 4 m Blanco telescope at the CTIO in the case of the southern fields (ELAIS-S1 and Chandra-S) or using MegaCam at the 3.6 m CFHT in the case of the northern fields (ELAIS-N1, ELAIS-N2, and Lockman). A summary of the latter observations and spectroscopic confirmation of two clusters at $z = 1.18$ and $z = 1.20$ in the ELAIS-N2 field may be found in the companion paper by Muzzin et al. (2009).

2.2. The CTIO Data Set

The SWIRE IRAC 3.6 μ m Southern fields are shown in Figure 1. The 3.6 μ m mosaic of the ELAIS-S1 field totals 7.1 deg² and the Chandra-S field totals 8.1 deg² (see Table 1).

The 8192 × 8192 pixel MOSAIC II camera on the 4 m Blanco telescope has a pixel scale of 0'.267 pixel⁻¹, leading to a 36' × 36' footprint per pointing. The white squares overlaid on Figure 1 show the 46 CTIO MOSAIC II pointings required to image the ELAIS-S1 and Chandra-S fields. These pointings were designed to maximize the overlap with the 3.6 μ m data, but to minimize the overall number of pointings by omitting regions with little overlap with the IRAC data. The total area of the z' observations per field is shown in Table 1.

CTIO observations were made of the ELAIS-S1 and Chandra-S fields using the z' filter on a total of 17 nights. The depth of the z' data varies from pointing to pointing depending on the seeing and the sky background; however, the mean depth is 24.0 AB (23.5 Vega; 5 σ). Table 1 shows the total effective area per field, i.e., the total usable area of overlap between the z' and 3.6 μ m data sets once areas of bright star contamination and chips gaps have been excluded. The total effective area of the CTIO fields is 13.6 deg² (6.5 deg² in the ELAIS-S1 and 7.1 deg² in the Chandra-S fields), and the total effective area of the six fields is 41.9 deg².

3. CLUSTER DETECTION

We defer a full description of the SpARCS data reduction, cluster candidate detection algorithm and catalogs to A. Muzzin et al. (2009, in preparation), and provide only a brief overview of the main details here. Photometry was performed on both the z' and IRAC mosaics using the SExtractor photometry package (Bertin & Arnouts 1996). The $z' - 3.6$ color (Column 6 in

¹⁵ <http://www.faculty.ucr.edu/~gillianw/SpARCS>

¹⁶ <http://www.cfht.hawaii.edu/Science/CFHTLS/>

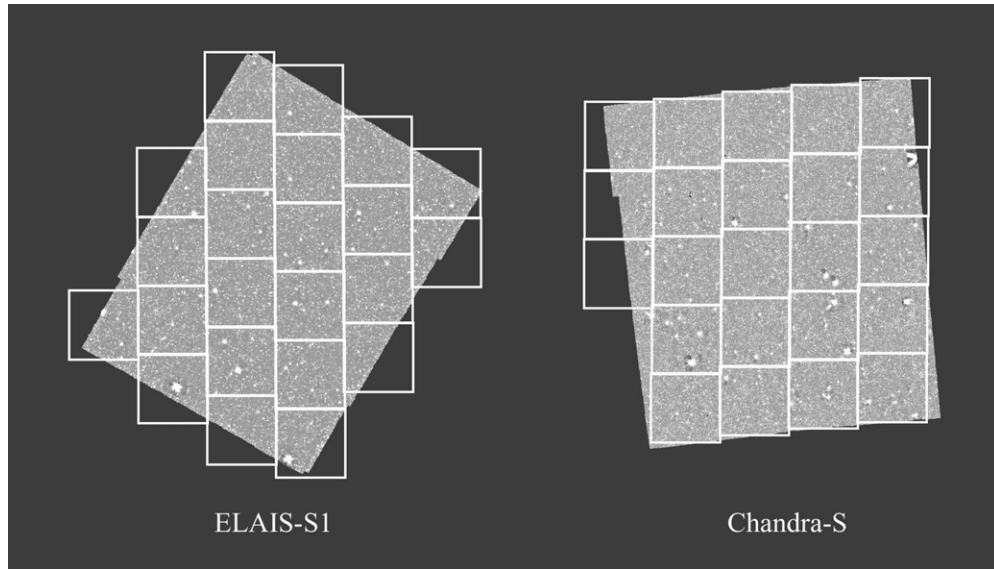


Figure 1. SWIRE 3.6 μm IRAC mosaics are shown in grayscale. The roll angle of *Spitzer* on the date of observation determines the orientation of the IRAC observations. The white squares overlaid show the 46 CTIO MOSAIC II pointings. There are 23 MOSAIC II pointings each in the SWIRE 7.1 deg^2 ELAIS-S1 and 8.1 deg^2 Chandra-S fields.

Table 2
Spectroscopic Redshifts in the Field of SpARCSJ0035.7–4312

ID	R.A. J2000 (Deg)	Decl. J2000 (Deg)	z' (Mag Vega)	3.6 μm (Mag Vega)	$z'-3.6 \mu\text{m}$ (Mag Vega)	z_{spec}
(1)	(2)	(3)	(4)	(5)	(6)	(7)
Members						
3	0.597095	-43.20612	21.59	15.77	5.45	1.329
4	0.596806	-43.20263	22.62	16.97	5.41	1.337
5	0.598068	-43.19822	22.19	16.36	5.45	1.315
6	0.596565	-43.19285	22.70	16.89	5.54	1.339
1001	0.596076	-43.21811	22.22	17.21	5.00	1.327
1002	0.596473	-43.21479	23.69	17.93	5.77	1.329
1009	0.597075	-43.20102	22.78	17.63	5.17	1.324
1010	0.597606	-43.20000	22.28	17.32	4.98	1.347
1012	0.596664	-43.19551	22.98	17.37	5.59	1.344
3002	0.597252	-43.21589	21.81	17.35	4.41	1.340
Foreground/Background						
1	0.599490	-43.20939	22.33	16.62	5.52	1.100
1007	0.598371	-43.20495	22.84	17.35	5.48	1.394
2010	0.599674	-43.21098	22.98	17.90	5.01	1.104
3003	0.598673	-43.21307	21.62	17.06	4.48	1.550
4001	0.596434	-43.19699	22.68	18.29	4.26	1.581

Notes. (4) z' magnitude in a $3''.66$ diameter aperture, (5) total 3.6 μm magnitude, and (6) $z' - [3.6]$ color in a $3''.66$ aperture with aperture correction.

Table 2) was computed using an aperture of diameter three IRAC pixels ($3''.66$). No aperture corrections were applied to the z' photometry because the $3''.66$ color aperture was much larger than the median seeing. However, the IRAC point-spread function has broad wings compared to a typical ground-based seeing profile, and it was necessary to apply an aperture correction to the measured 3.6 μm magnitude before computing the color of each galaxy. Total 3.6 μm magnitudes (Column 5 in Table 2) were computed using a large aperture, equal to the geometric mean radius of the isophotal aperture determined by SExtractor (see also Lacy et al. 2005 and Muzzin et al. 2008).

Clusters are identified using the red-sequence cluster method (Gladders & Yee 2000, 2005), which maps the density of

galaxies in a survey within narrow color slices and flags the highest overdensities as candidate clusters. We note that the detection algorithm used for the SpARCS survey is almost identical to that described in Muzzin et al. (2008), as applied to the *Spitzer* First Look Survey (FLS; Lacy et al. 2005; Wilson et al. 2006). The one important difference is that Muzzin et al. (2008) used an $R - [3.6]$ color to detect clusters at $0 < z < 1.3$ in the FLS. The slightly deeper SWIRE exposure time, combined with the $z' - [3.6]$ color choice, allows SpARCS to detect clusters to higher redshift than possible with the FLS data set.

3.1. SpARCS J003550–431224

From analysis of the ELAIS-S1 field, SpARCS J003550–431224, shown in Figure 2, was identified as a high probability rich cluster candidate.

A parameter that is commonly used to quantify the richness of a cluster is B_{gc} , the amplitude of the three-dimensional, cluster center-galaxy spatial correlation function (Yee & López-Cruz 1999). The B_{gc} statistic is relatively easy to apply as it involves counting galaxies, and it is, modulo statistical fluctuations, independent of the counting aperture and the survey magnitude limit, allowing a straightforward comparison between the richnesses of clusters selected from different surveys. Gladders & Yee (2005) introduced the $B_{\text{gc,R}}$ richness parameter, the amplitude of the three-dimensional, cluster center-*red-sequence*-galaxy spatial correlation function. SpARCS J003550–431224 (R.A.: 00:35:49.7, decl.: -43:12:24.16) has a $B_{\text{gc,R}}^{17}$ richness of $1055 \pm 276 \text{ Mpc}^{1.8}$. Based on the empirical calibration of B_{gc} versus M_{200} determined by Muzzin et al. (2007) in the K band for the CNOC1 clusters at $z \sim 0.3$, this implies $M_{200} = 5.7 \times 10^{14} M_{\odot}$.

4. SPECTROSCOPY

Spectroscopic follow-up of SpARCS J003550–431224 was obtained with the Gemini Multi-Object Spectrograph on the Gemini South telescope (GMOS-S) in queue mode (program

¹⁷ We use the $z' - [3.6]$ versus 3.6 μm red sequence to determine $B_{\text{gc,R}}$.

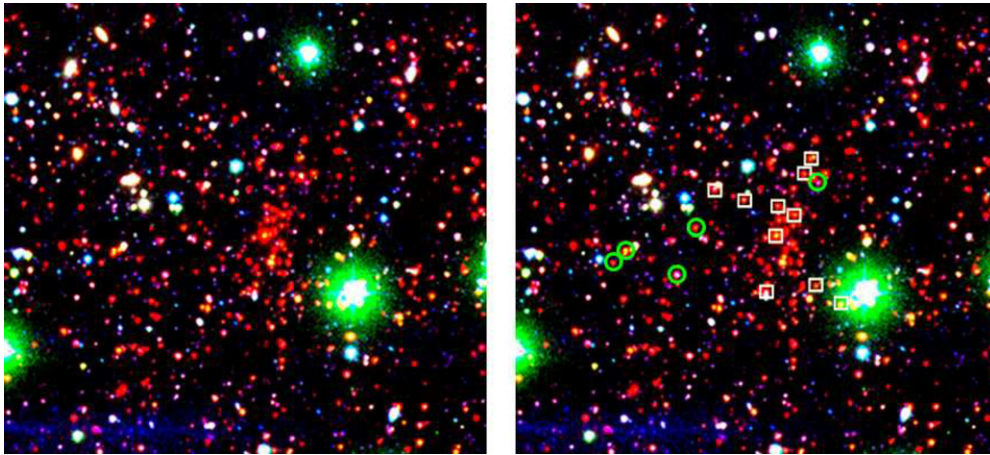


Figure 2. Here $r'z'[3.6]$ color composites of J003550–431224 are shown in both panels. The field of view (FOV) is $5'$ (2.5 Mpc at the cluster redshift). The white squares (green circles) overlaid on the right panel show the 10 cluster members (five foreground/background galaxies) with spectroscopically confirmed redshifts from Gemini/GMOS-S (see Table 2).

ID GS-2007B-Q16). We used $1''$ wide slits. We used GMOS with the R150 grism, blazed at 7170 \AA . This provided a spectral resolving power of $R = 631$ which corresponds to a resolution of 11 \AA , or 280 km s^{-1} at the redshift of the cluster.

We observed a single mask for 10 hr. The mask was observed using the OG515 filter which blocks light blueward of 5150 \AA . The central wavelength of the grating was moved between 7380 \AA , 7500 \AA , and 7620 \AA to “dither” in the dispersion direction and fill in GMOS chip gaps. We used nod-and-shuffle in band-shuffle mode. This is slightly less efficient than micro-shuffle mode but allows one to maximize the number of slits in a small area, such as is the case for a distant cluster with a high surface density of red-sequence galaxies concentrated in the cluster core (see Figure 2). There were 26 slits on the mask, including three alignment stars.

To reduce the number of slits placed on obvious foreground galaxies, we prioritized slits on galaxies with colors near the cluster red sequence. To avoid significant selection bias, we used a very broad cut around the red sequence, intended to include both star-forming and non-star-forming systems. Slits were placed on galaxies with priorities from 1 to 5. Priority 1 (single digit ID nos. in Table 2) was galaxies with colors within 0.6 mag of the red sequence, and with $[3.6] < 17.0$ (Vega). Priority 2 (ID nos. in the 1000’s) was galaxies with colors within 0.6 mag of the red sequence, and with $17.0 < [3.6] < 18.0$. Priority 3 (ID nos. in the 2000’s) was galaxies with colors bluer than the red sequence by 0.6–1.0 mag, and with $[3.6] < 17.5$. Priority 4 (ID nos. in the 3000’s) was galaxies with colors bluer than the red-sequence by 1.0–1.5 mag, and with $[3.6] < 17.5$. Priority 5 (ID nos. in the 4000’s) was the lowest priority and included all galaxies with magnitude $16.9 < [3.6] < 18.0$. Priorities 1–4 roughly correspond to bright red-sequence, faint red-sequence, blue cloud, and extreme blue cloud galaxies, respectively. Each exposure was 30 minutes in duration. The 20 exposures used nod cycles of 60 s integration time per cycle and were offset by a few arcseconds using the on-chip dithering option.

4.1. Data Reduction

The data were reduced using standard GeminiIRAF routines to bias-subtract the data. The iGDDS package (Abraham et al. 2004) was used to interactively trace the two-dimensional spectra and extract one-dimensional spectra. Wavelength calibration

for each extracted spectrum was performed—using bright sky lines from the unsubtracted image, also with the iGDDS software. Wavelength solutions typically have an rms $< 0.5 \text{ \AA}$. We determined a relative flux calibration curve using a long slit observation of the standard star EG21. We determined redshifts by identifying prominent spectra features such as calcium H+K lines at 3934 \AA and 3968 \AA and the $[\text{O II}] \lambda\lambda 3727$ doublet using the iGDDS code. A few of the spectra also show some Balmer series lines.

Spectra were obtained for 15 of the 23 photometrically selected galaxies with quality sufficient for determining redshifts: the other eight were deemed too faint for reliable identification of spectral features. Table 2 shows 10 galaxies, which were deemed likely to be cluster members based upon the value of their spectroscopic redshifts (although see Section 5). These galaxies are indicated by white boxes in the right panel of Figure 2. Some examples of the spectra of confirmed members are shown in Figure 3. These spectra have been smoothed by a 7 pixel boxcar (which produces a resolution equal to that of the spectrograph).

A total of five galaxies were determined to be foreground or background sources. These galaxies are also listed in Table 2 and indicated by green boxes in the right panel of Figure 2. The histogram in the left panel of Figure 4 shows the spectroscopic redshifts of all 15 galaxies. The histogram in the right panel shows only the redshifts of the 10 likely cluster members.

5. DISCUSSION

Before calculating a redshift and velocity dispersion for SpARCS J003550–431224, we first checked for near-field interlopers using the code of Blindert (2006). This code employs a modified version of the Fadda et al. (1996) shifting-gap technique, which uses both galaxy position and velocity information to reject interlopers. Figure 5 shows galaxy velocities relative to the mean velocity, as a function of radius. The galaxy marked with an “x” (ID 5 at $z = 1.315$ in Table 2) was identified as being more likely to be a near-field object than a member of the cluster and was not used in the computation of the velocity dispersion or the mean redshift of the cluster. (This is also the lowest redshift galaxy in the right panel of Figure 4.)

Once cluster membership was established, both the redshift and velocity dispersion, σ_v , of SpARCS J003550–431224 were then calculated iteratively using the “robust estimator,” σ_{rob}

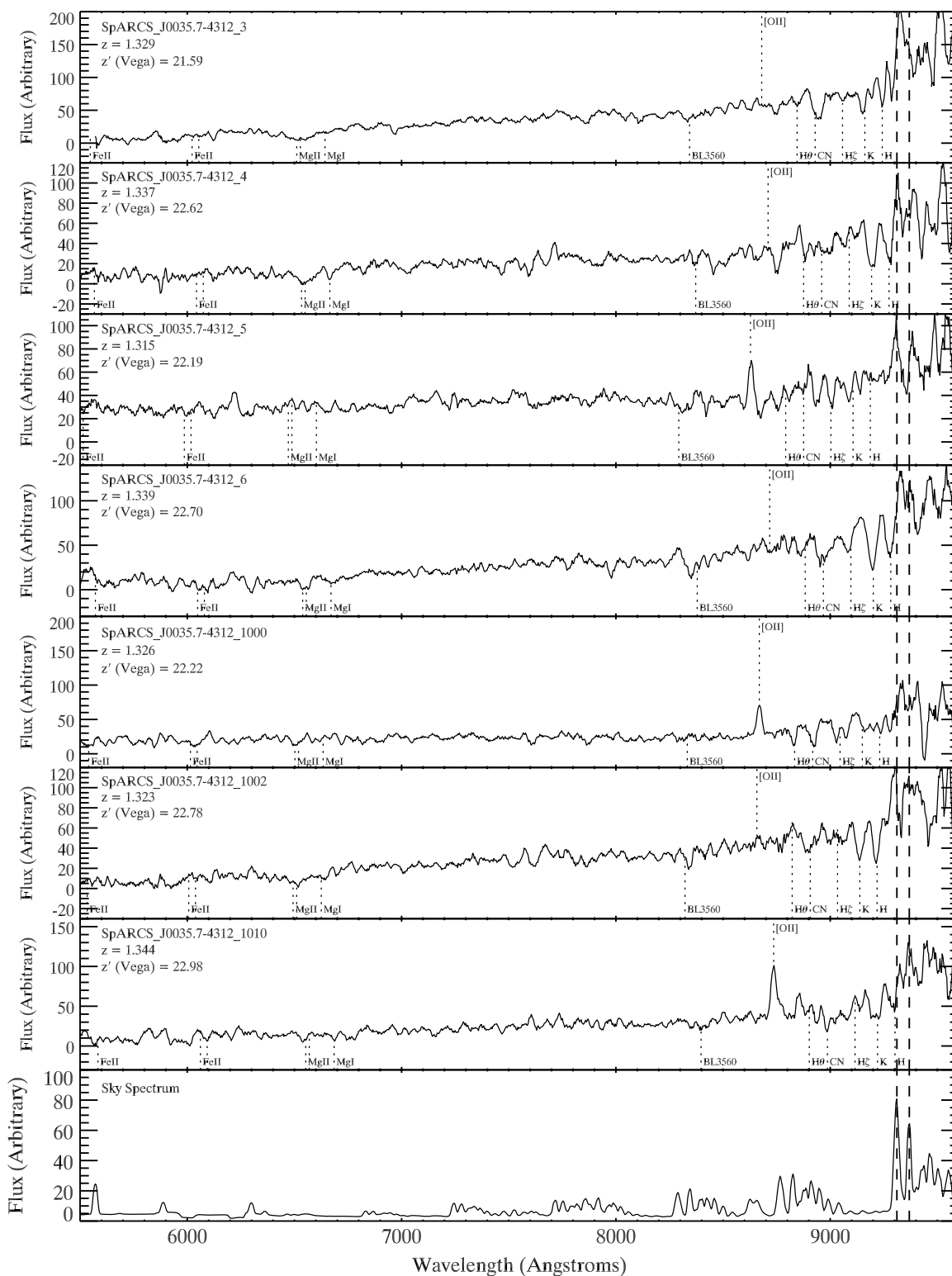


Figure 3. Spectra for a subsample of seven galaxies in cluster SpARCS J003550–431224 (see Table 2). The spectra have been smoothed with a 7 pixel (11 \AA) boxcar. The identified spectral features are marked. The lowermost panel shows the typical sky spectrum.

(Beers et al. 1990). The robust estimator has been shown to be less sensitive than the standard deviation to outliers which may persist even after rejecting interlopers using the shifting-gap technique. The actual estimator used depends on the number of cluster members and is either the biweight estimator for data sets with at least 15 members, or, as in this case, the gapper

estimator which has been shown to be the most robust choice in the case of data sets with fewer than 15 members. Both the biweight and gapper estimator are discussed more fully in Beers et al. (1990) and Blindert (2006).

A mean redshift of $z = 1.335$ and a velocity dispersion of $1050 \pm 230 \text{ km s}^{-1}$ were calculated for SpARCS

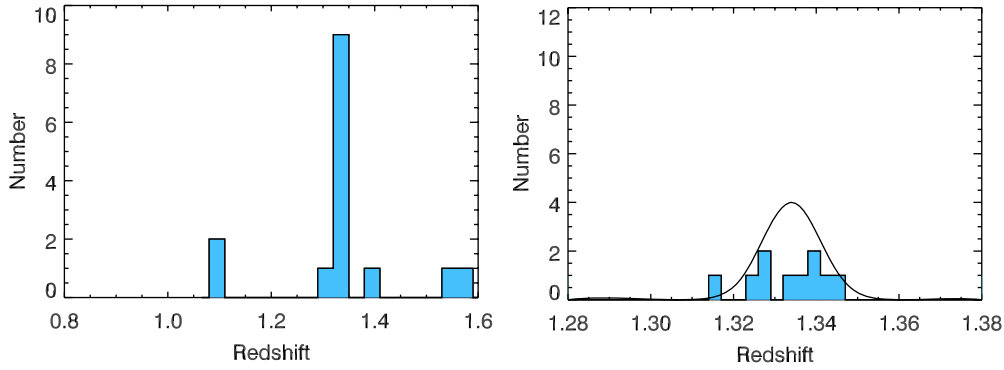


Figure 4. Histogram showing 15 galaxies with confirmed redshifts (left). Ten galaxies are confirmed as cluster members (right) and five are confirmed as foreground or background sources. See Table 2 for further details. A Gaussian with an rms of 1050 km s^{-1} (see Section 5) has been overlaid. (A color version of this figure is available in the online journal.)

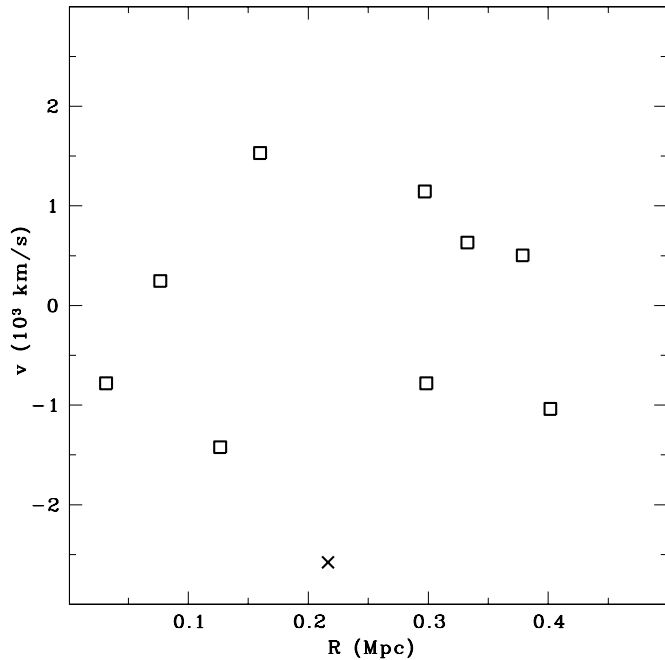


Figure 5. Galaxy velocities relative to the mean velocity, as a function of radius. The galaxy marked with an “x” (ID no. 5 at $z = 1.315$ in Table 2) is more likely to be a near-field object than a member of the cluster and was not used in the computation of the mean redshift or velocity dispersion.

J003550–431224. The uncertainty on the latter was determined using Jackknife resampling of the data. Due to the small number of confirmed members it is, as yet, unclear as to whether SpARCS J003550–431224 is a relaxed cluster or a system in the process of collapsing. Nonetheless, for comparison, a Gaussian with an rms of 1050 km s^{-1} has been overlaid on the right panel of Figure 4. The velocity dispersion of $1050 \pm 230 \text{ km s}^{-1}$ should certainly be considered “preliminary,” based, as it is, upon only nine members. However, if one does adopt this value of velocity dispersion, one can use it to calculate a dynamical estimate of r_{200} (the radius at which the mean interior density is 200 times the critical density, ρ_c) using the equation of Carlberg et al. (1997):

$$r_{200} = \frac{\sqrt{3}\sigma}{10H(z)}, \quad (1)$$

where $H(z)$ is the Hubble parameter at the redshift of the cluster. This gives a value of $r_{200} = 1.2 \pm 0.3 \text{ Mpc}$. From this, the

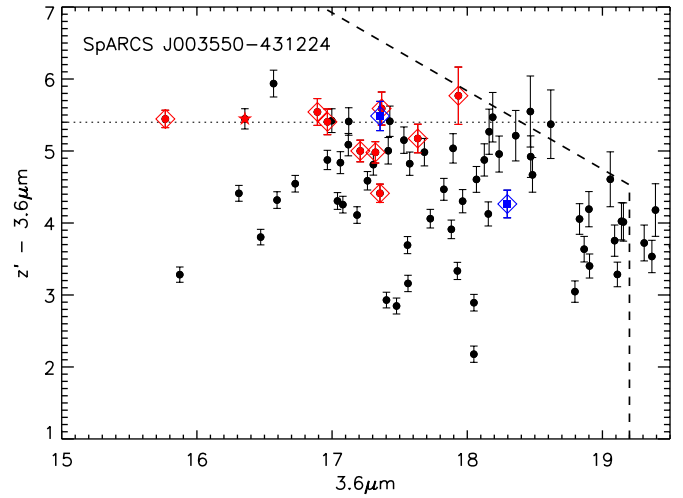


Figure 6. $z' - [3.6]$ vs. $[3.6]$ color–magnitude diagram for SpARCS J003550–431224. The black circles are all the galaxies contained within a circle of radius 550 kpc ($65''$) at the cluster redshift. The red symbols show the 10 galaxies from Figure 5. The red diamonds denote the nine galaxies used in the computation of the velocity dispersion (shown as boxes in Figure 5), and the red star denotes the galaxy identified as a near-field object (cross in Figure 5). The blue squares show the two (of five) confirmed foreground/background galaxies which fall within the 550 kpc radius. The dotted line indicates the nominal red-sequence color for this cluster ($z' - [3.6] = 5.4$). See Section 5 for a discussion. (A color version of this figure is available in the online journal.)

dynamical mass M_{200} , the mass contained within r_{200} , can also be inferred using

$$M_{200} = \frac{4}{3}\pi r_{200}^3 \times 200\rho_c. \quad (2)$$

We estimate a dynamical mass of $M_{200} = (9.4 \pm 6.2) \times 10^{14} M_\odot$ for J003550–431224, which is in good agreement with, albeit slightly larger than, the value of $M_{200} = 5.7 \times 10^{14} M_\odot$, which was calculated based upon its richness. Further spectroscopy is certainly warranted, but the preliminary evidence suggests that SpARCS J003550–431224 is a massive cluster, perhaps the most massive cluster at $z > 1$ in our 42 deg^2 survey.

The color–magnitude diagram for all galaxies in a 550 kpc ($65''$) radius of the cluster center is shown in Figure 6. The red symbols show the 10 cluster members from Table 2. The blue squares show the two (of five) confirmed foreground/background galaxies that fall within the 550 kpc radius.

Based on its red-sequence color of $z' - [3.6] = 5.4$ (shown as dotted line in Figure 6), SpARCS J003550–431224 was

originally assigned a photometric redshift of $z = 1.57$. This was based on Bruzual & Charlot (BC03; 2003) models assuming a formation redshift $z_f = 4$. If one assumes a formation redshift of $z_f = 10$, then the $z' - [3.6] = 5.4$ color would cause one to infer a photometric redshift of $z = 1.39$ for SpARCS J003550–431224, which is reasonably consistent with the spectroscopic value. One possibility for the overestimate of the photometric redshift is that the BC03 models are too blue at young ages, as suggested by Maraston (2005). (We note that a recent paper by Mei et al. 2009 found a similar effect for the colors of galaxies in the two primary clusters, RX J0848.9+4452 and RX J0848+4453, of the Lynx supercluster at $z = 1.27$.) Spectroscopy of additional $z \sim 1.35$ SpARCS clusters will determine whether SpARCS J003550–431224's red-sequence color is representative for this redshift, or if there is something atypical about this particular cluster.

6. CONCLUSIONS

The complete SpARCS catalog contains *hundreds* of cluster candidates at $z > 1$ and promises to be one of the premier data sets for the study of cluster galaxy evolution at $z > 1$. In this paper, we reported the discovery of SpARCS J003550–431224 in the ELAIS-S1 field, a very rich galaxy cluster at $z = 1.335$, with a preliminary velocity dispersion of $1050 \pm 230 \text{ km s}^{-1}$. Several other rich $z > 1$ clusters in the SpARCS survey have also been spectroscopically confirmed (Muzzin et al. 2009; R. Demarco et al. 2009, in preparation), with no false positives.

The FLS, IRAC Shallow Cluster Survey (ISCS), and SpARCS have demonstrated the power and potential of widefield infrared observations from space for $z > 1$ cluster surveys. Both the FLS and SpARCS surveys are very similar to the RCS-1 and RSC-2 surveys, except that they utilize an optical-infrared adaptation of the CRS technique (the ISCS uses a multipassband photometric technique). SpARCS, in particular, is a demonstration that we have entered an era when it is possible to select large numbers of $z > 1$ clusters homogeneously, using relatively modest observational resources. With its two filter red-sequence detection algorithm, our technique is both highly efficient and robust against line-of-sight projections. At 42 deg^2 , the SpARCS survey is also currently the only $z > 1$ survey containing sufficiently large numbers of clusters to permit simultaneously subdividing the catalog, and studying cluster evolution as a function of *both* redshift and richness.

It is noteworthy that all the $z > 1$ SpARCS clusters were discovered in only 120 s per pointing of IRAC observations. Since clusters are rare, widefield cluster searches are required to discover the most massive examples. To discover a representative sample of massive structures at $z > 1.5$ would require an even wider survey, of several hundred square degrees, a proposition which would be feasible during the lifetime of the *Spitzer* Warm Mission (Gardner et al. 2007; Stauffer et al. 2007).

The authors thank the staff of The Cerro Tololo Inter-American Observatory for their invaluable assistance, without which this work would not have been possible. CTIO is operated by the Association of Universities for Research in Astronomy, under contract with the National Science Foundation.

Based on observations obtained at the Gemini Observatory, which is operated by the Association of Universities for Research in Astronomy, Inc., under a cooperative agreement with the NSF on behalf of the Gemini partnership: the National Science Foundation (US), the Science and Technology Facilities

Council (UK), the National Research Council (Canada), CONICYT (Chile), the Australian Research Council (Australia), Ministério da Ciência e Tecnologia (Brazil) and SECYT (Argentina).

This work is based in part on archival data obtained with *Spitzer*, which is operated by the Jet Propulsion Laboratory, California Institute of Technology under a contract with NASA. Support for this work was provided by an award issued by JPL/Caltech. G.W. acknowledges support from the College of Natural and Agricultural Sciences at UCR.

REFERENCES

- Abell, G. O. 1958, *ApJS*, 3, 211
 Abraham, R. G., et al. 2004, *AJ*, 127, 2455
 Beers, T. C., Flynn, K., & Gebhardt, K. 1990, *AJ*, 100, 32
 Bertin, E., & Arnouts, S. 1996, *A&AS*, 117, 393
 Blakeslee, J. P., et al. 2003, *ApJ*, 596, L143
 Blindert, K. 2006, PhD thesis, Univ. Toronto
 Bower, R. G., Lucey, J. R., & Ellis, R. S. 1992, *MNRAS*, 254, 601
 Brodwin, M., et al. 2006, *ApJ*, 651, 791
 Bruzual, G., & Charlot, S. 2003, *MNRAS*, 344, 1000
 Carlberg, R. G., et al. 1997, *ApJ*, 485, L13
 Dalton, G. B., et al. 2006, Proc. SPIE, 6269, 62690x
 Donahue, M., Voit, G. M., Gioia, I., Lupino, G., Hughes, J. P., & Stocke, J. T. 1998, *ApJ*, 502, 550
 Eisenhardt, P. R. M., et al. 2004, *ApJS*, 154, 48
 Eisenhardt, P. R. M., et al. 2008, *ApJ*, 684, 905
 Fadda, D., Girardi, M., Giuricin, G., Mardirossian, F., & Mezzetti, M. 1996, *ApJ*, 473, 670
 Fazio, G. G., et al. 2004, *ApJS*, 154, 10
 Gardner, J. P., Fan, X., Wilson, G., & Stiavelli, M. 2007, in AIP Conf. Ser. 943, The Science Opportunities of the Warm Spitzer Mission Workshop, ed. L. J. Storrie-Lombardi & N. A. Silbermann (Melville, NY: AIP), 229
 Gilbank, D. G., Yee, H. K. C., Ellingson, E., Gladders, M. D., Barrientos, L. F., & Blindert, K. 2007, *AJ*, 134, 282
 Gioia, I. M., Henry, J. P., Maccacaro, T., Morris, S. L., Stocke, J. T., & Wolter, A. 1990, *ApJ*, 356, L35
 Gioia, I. M., & Luppino, G. A. 1994, *ApJS*, 94, 583
 Gladders, M. D., & Yee, H. K. C. 2000, *AJ*, 120, 2148
 Gladders, M. D., & Yee, H. K. C. 2005, *ApJS*, 157, 1
 Gonzalez, A. H., Zaritsky, D., Dalcanton, J. J., & Nelson, A. 2001, *ApJS*, 137, 117
 Holden, B. P., Stanford, S. A., Eisenhardt, P., & Dickinson, M. 2004, *AJ*, 127, 2484
 Koester, B. P., et al. 2007a, *ApJ*, 660, 239
 Koester, B. P., et al. 2007b, *ApJ*, 660, 221
 Lacy, M., et al. 2005, *ApJS*, 161, 41
 Lidman, C., et al. 2008, *A&A*, 489, 981
 Lonsdale, C. J., et al. 2003, *PASP*, 115, 897
 Maraston, C. 2005, *MNRAS*, 362, 799
 Mei, S., et al. 2009, *ApJ*, 690, 42
 Muzzin, A., Wilson, G., Lacy, M., Yee, H. K. C., & Stanford, S. A. 2008, *ApJ*, 686, 966
 Muzzin, A., Yee, H. K. C., Hall, P. B., & Lin, H. 2007, *ApJ*, 663, 150
 Muzzin, A., et al. 2009, *ApJ*, 698, 1934
 Postman, M., Lauer, T. R., Szapudi, I., & Oegerle, W. 1998, *ApJ*, 506, 33
 Postman, M., Lubin, L. M., Gunn, J. E., Oke, J. B., Hoessel, J. G., Schneider, D. P., & Christensen, J. A. 1996, *AJ*, 111, 615
 Rieke, G. H., et al. 2004, *ApJS*, 154, 25
 Rosati, P., della Ceca, R., Norman, C., & Giacconi, R. 1998, *ApJ*, 492, L21
 Rosati, P., Stanford, S. A., Eisenhardt, P. R., Elston, R., Spinrad, H., Stern, D., & Dey, A. 1999, *AJ*, 118, 76
 Stanford, S. A., et al. 2005, *ApJ*, 634, L129
 Stauffer, J. R., et al. 2007, in AIP Conf. Ser. 943, The Science Opportunities of the Warm Spitzer Mission Workshop, ed. L. J. Storrie-Lombardi & N. A. Silbermann (Melville, NY: AIP), 43
 Surace, J., Shupe, D. L., Fang, F., Lonsdale, C. J., & Gonzalez-Solares, E. 2005, SSC Web site Release: SWIRE Data Release 2 (Pasadena, CA: Caltech), http://swire.ipac.caltech.edu/swire/astronomers/publications/SWIRE2_doc_083105.pdf
 Warren, S. J., et al. 2007, *MNRAS*, 375, 213
 Werner, M. W., et al. 2004, *ApJS*, 154, 1

- White, S. D. M., et al. 2005, *A&A*, **444**, 365
- Wilson, G., Muzzin, A., Lacy, M., & the FLS Team 2006, in ASP Conf. Ser. 357, *The Spitzer Space Telescope: New Views of the Cosmos*, ed. L. Armus & W. T. Reach (San Francisco, CA: ASP), 238
- Wilson, G., et al. 2008, in ASP Conf. Ser. 381, *Infrared Dignostics of Galaxy Evolution*, ed. R.-R. Chary, H. I. Teplitz, & K. Sheth (San Francisco, CA: ASP), 210
- Yee, H. K. C., Ellingson, E., & Carlberg, R. G. 1996, *ApJS*, **102**, 269
- Yee, H. K. C., Gladders, M. D., Gilbank, D. G., Majumdar, S., Hoekstra, H., & Ellingson, E. 2007, in ASP Conf. Ser. 379, *Cosmic Frontiers*, ed. N. Metcalfe & T. Shanks (San Francisco, CA: ASP), 103
- Yee, H. K. C., & López-Cruz, O. 1999, *AJ*, **117**, 1985
- Zwicky, F., Herzog, E., & Wild, P. 1968, *Catalog of Galaxies and of Clusters of galaxies* (Pasadena, CA: Caltech; 1961–1968)